Research Square

Preprints are preliminary reports that have not undergone peer review.
They should not be considered conclusive, used to inform clinical practice,
or referenced by the media as validated information.

Development and Optimization of Puerarin-loaded ion-triggered in situ gel for ocular delivery in dry eye disease

Kiran B. Dhamak

kirandhamak21@gmail.com

PRES's College of Pharmacy (For Women)

Kiran B. Kotade

PRES's College of Pharmacy (For Women)

Sachin B. Somwanshi

PRES's College of Pharmacy (For Women)

Vinayak M. Gaware

PRES's College of Pharmacy (For Women)

Rahul D. Khaire

PRES's College of Pharmacy (For Women)

Research Article

Keywords: Puerarin, Ion-triggered in situ gel, Dry eye disease, Gellan gum, Tamarind seed xyloglucan, Ocular drug delivery, 3^2 Factorial design, Mucoadhesion

Posted Date: October 22nd, 2026

DOI: https://doi.org/10.21203/rs.3.rs-10687819/v1

License: This work is licensed under a Creative Commons Attribution 4.0 International License. Read Full License

Additional Declarations: No competing interests reported.

Abstract

Objectives

Dry eye disease is a prevalent ophthalmic disorder with limited therapeutic outcomes from conventional eye drops due to rapid precorneal drainage and poor ocular bioavailability. This study aimed to develop, optimize, and characterize a puerarin-loaded ion-triggered in situ gel for sustained ocular delivery in dry eye disease management.

Methods

Formulations were prepared using gellan gum as the primary ion-sensitive gelling polymer and tamarind seed xyloglucan as a novel mucoadhesive excipient. A 3^2 full factorial design optimized two independent variables, gellan gum (X_1: 0.3, 0.5, 0.7% w/v) and tamarind seed xyloglucan (X_2: 0.1, 0.2, 0.3% w/v), against gelation pH, mucoadhesive strength, and ex vivo corneal permeation at 8 hours as dependent responses.

Results

Quadratic and 2FI models demonstrated excellent predictive accuracy (adjusted R^2 up to 0.9989). Batch F8 was selected as the optimized formulation based on the highest composite desirability score (0.920), achieving gelation pH 7.4 ± 0.02, mucoadhesive strength 604.7 ± 7.45 dynes/cm², cumulative drug release 82.42% at 12 hours, and Papp 0.768×10^{-3} cm/h. Drug release followed anomalous non-Fickian transport (n = 0.7815, R^2 = 0.9995). Accelerated stability confirmed physicochemical robustness over six months per ICH Q1A(R2).

Conclusion

The optimized puerarin-loaded ion-triggered in situ gel demonstrated sustained precorneal drug delivery with superior mucoadhesion and corneal permeation, offering a clinically viable alternative to conventional ophthalmic drops with strong potential for future clinical translation.

Introduction

Dry Eye Disease (DED) constitutes among the most common ocular surface disorders globally; its incidence ranges between 5% and 50% according to different diagnostic criteria and geographical regions, with particularly high rates noted within Asia [1, 2]. Characterization of this disorder includes tear film instability, elevated osmolality, inflammatory processes at the ocular surface, and sensory abnormalities that result in marked visual disability and reduction of quality of life [3, 4]. Economic burden attributable to DED is considerable and exceeds billions annually because of repeated medical consultations and pharmacologic intervention along with losses in labor productivity. Currently employed standards of care include application of artificial tears, steroids, emulsion containing ciclosporin A and lifitegrast ophthalmic solutions; these therapies afford symptomatic alleviation yet fail to address underlying pathology adequately. Standard eyedrops predominate in pharmaceutical markets and exhibit deficiencies such as rapid drainage into nasolacrimal duct, reflex secretion and short duration of corneal contact thereby resulting in more than 95% loss of applied doses before reaching precorneal site [5]. Such shortcomings highlight an imperative requirement for innovation directed toward development of new strategies for ocular drug

delivery aimed at increasing residence times of therapy and ensuring prolonged release while improving patient adherence.

Puerarin, which is extracted mainly from roots of Pueraria lobata (known also as Kudzu) and exists as a glucoside of flavones possessing chemical formula C21H20O9 and molecular weight of 416.38 g/mol with good aqueous solubility and stability within physiological pH range, emerges as an important therapeutic agent for the management of DED [6]. Mechanisms responsible for therapeutic efficacy include potent suppression of pro inflammatory cytokines such as interleukin 1 β (IL-1β), interleukin 6 (IL-6) and tumor necrosis factor α (TNF α) [7, 8]. Antioxidant activities are achieved through scavenging reactive oxygen species. Additionally, puerarin promotes corneal epithelium cell proliferation and restoration of goblet cell density [9, 10]. Clinical preclinical and experimental results show effective reduction of ocular surface inflammation, diminution of apoptosis among corneal epithelial cells and restoration of tear secretion in animal model experiments using puerarin [11, 12]. Furthermore, puerarin demonstrates favorable tolerance of the eye but suffers from established limitations related to low permeability of cornea, rapid clearance from precorneal sites and insufficient levels of active drug at target tissues; therefore development of innovative formulation approaches is necessary to realize full therapeutic potential of this compound [13, 14].

Ion triggered systems that undergo gel formation in situ serve as highly promising platforms for delivery of drugs to the eye; they initiate phase transitions when instilled into the conjunctival cul de sac by virtue of physiological ions including sodium and calcium ions found in tear fluid. Prepared initially as low viscosity aqueous solutions, these systems display facile administration akin to traditional eye drops yet transform into viscoelastic gel matrices on contacting ocular surface thereby greatly extending retention times and improving bioavailability [15, 16]. Gelatin gum which is an anionic polysaccharide derived from microbial sources serves as the major sensitive gelling polymer within these systems due to its capacity to produce strong gels under physiologically relevant ionic concentrations [17, 18]. Resultant depot gel provides for regulated and sustained drug release reducing dosing frequency minimizing systemic uptake and markedly improving patient compliance. Recent developments within this field also include incorporation of other polymers to enhance mucosal adhesion gel strength and kinetic profiles thus strengthening scientific justification for adoption of this delivery system [19, 20].

This research intends to advance development and optimization of a gel formulation loaded with puerarin for ocular administration in management of dry eye disease [21, 22]. Specific goals include formulating using gellan gum as principal agent for gel formation, conducting systematic optimization of key quality attributes by means of experimental design methodology, thorough physicochemical characterization, assessment of permeation from excised corneas and evaluation of therapeutic efficacy employing models experimentally induced with dry eye disease [23, 24].

Materials and Methods

Materials

Puerarin (98.5% purity, molecular weight 416.38 g/mol) was acquired from Sciquaint Innovations Pvt. Ltd., Pune, India. Obtained also from Sciquaint Chemicals, Pune, India is gellan gum of low acylation grade having viscosity ranging between 85 and 115 mPa·s in aqueous solutions at concentration of 1%; pharmaceutical grade tamarind seed xyloglucan with molecular weight of approximately 800 kDa. From Research Lab Fine Chems Industries, Mumbai, India supply HPMC E4 M of United States Pharmacopeia grade having viscosities within range of 3000 to 5600 mPa·s in aqueous solutions at concentration of 2% along with mannitol of United States Pharmacopeia grade

having molecular weight of 182.17 g/mol and purity level of 99.0%. Benzalkonium chloride of analytical grade possessing purity of 95.0% together with disodium ethylenediaminetetraacetic acid of analytical grade having molecular weight of 372.24 g/mol and purity of 99.0% was purchased from Neeta Chemicals, Pune India. Potassium bromide of spectroscopic grade exhibiting purity of 99.5% and propylene glycol of pharmaceutical quality showing purity of 99.5% was obtained from Sciquaint Chemicals, Pune India. In house freshly prepared simulated tears involved sodium chloride, sodium bicarbonate, calcium chloride dihydrate and potassium chloride all being of analytical grade sourced from Research Lab Fine Chems Industries, Mumbai. Other chemicals and reagents utilized throughout study were of analytical grade and employed without further purification.

Methods

Calibration Curve of Puerarin

A calibration curve has been constructed utilizing simulated tears (STF; pH 7.4) for quantitation of puerarin concentrations in all subsequent analytical studies. A stock solution of puerarin at 1000 µg/mL (µg/mL) was prepared through dissolution of an accurate weight of pure substance into minimal volumes of methanol followed by dilution with STF [25, 26]. Working standard solutions ranging between 2 and 20 µg/mL were produced by serial dilutions. Absorbance was measured at λmaximum at wavelength 250 nm employing a UV visible spectrophotometer (Labman Scientific Instruments; LMSP UV1200; India). Linearity assessment involved plotting absorbance against concentration and derivation of regression equation. Measurements were made in triplicate (n = 3).

Fourier Transform Infrared Spectroscopy (FTIR)

Functional groups and possible drug excipient interactions were identified through Fourier Transform Infrared Spectroscopy studies on both pure puerarin and on physical mixtures. Samples were prepared by mixing about 2 mg of substance with 200 mg of dry potassium bromide and pressing them into translucent pellets under pressure of ten tons using a hydraulic press. Spectra were recorded employing an infrared spectrophotometer (Shimadzu IR Affinity-1 S made in Japan), recording spectra from a wave number range of 4000 to 400 cm to the minus one power at a resolution of 4 cm to the minus one power; 32 scans were collected for each sample. Peaks characteristic of puerarin and individual excipients were interpreted and compared among samples that are pure drug and physical mixtures to discern any spectral shift or disappearance related to interaction.

Solubility Study

Equilibrium solubility of puerarin has been determined in distilled water, simulated tears fluid which is buffered at pH 7.4 and PBS which also buffers at pH 6.8. An excess amount of drug approximately equal to 10 mg was added to 10 mL of each of these solvents into sealed glass vials and subjected to constant agitation using orbital shaker Remi Instruments model RS-12R operating at temperature of 25 ± 0.5°C and rotation speed of 100 rpm for a duration of 72 h until equilibrium was achieved. Following filtration through filters having pores of 0.45 µm and appropriate dilution samples were assayed spectrophotometrically at wavelength 250 nm. Results obtained have been reported as mean plus standard deviation mg/mL (n = 3).

Experimental Design

A full factorial design employing 3^2 was used for systematic optimization of gel formulation that entraps puerarin [27, 28]. Selection was made of two independent variables namely concentration of gellan gum (X_1) which is a primary sensitive ion gelling polymer and concentration of xyloglucan from Tamarind seeds (X_2) which is an innovative mucoadhesive polysaccharide (Table 1). Both variables were examined at three levels; low negative (-1), zero (0) and positive high (+ 1); thereby resulting in nine different formulated samples designated F1 through F9 (Table 2).

The general polynomial equation applied was:

$$Y = b_0 + b_1X_1 + b_2X_2 + b_{12}X_1X_2 + b_{11}X_1^2 + b_{22}X_2^2$$

For Y representing the response of dependent variable, b sub zero serves as intercept while b_1 and b_2 denote regression coefficients relating to additive effects of gellan gum and xyloglucan from seeds of tamarind respectively [29, 30]. Moreover, b_{12} denotes an interaction coefficient whereas b_{11} and b_{22} represent quadratic coefficients. Response surface modeling and statistical analysis were performed using Design Expert software version 13.0 of Stat Ease Inc in the United States.

Table 1
Independent and Dependent Variables in 3^2 Factorial Design

Variable	Level – 1 (Low)	Level 0 (Medium)	Level + 1 (High)
Independent Variables			
X_1: Gellan gum (% w/v)	0.3	0.5	0.7
X_2: Tamarind seed xyloglucan (% w/v)	0.1	0.2	0.3
Dependent Variables			**Goal**
Y_1: Gelation temperature (°C)			Minimize
Y_2: Drug release at 8h (%)			Maximize (≥ 80%)
Y_3: Mucoadhesive force (dyne/cm²)			Maximize

Table 2
Formulation Table for Puerarin-Loaded Ion-Triggered In Situ Gel (F1–F9)

Ingredient	F1	F2	F3	F4	F5	F6	F7	F8	F9
Puerarin (mg)	10	10	10	10	10	10	10	10	10
Gellan gum (% w/v)	0.3	0.5	0.7	0.3	0.5	0.7	0.3	0.5	0.7
Tamarind seed xyloglucan (% w/v)	0.1	0.1	0.1	0.2	0.2	0.2	0.3	0.3	0.3
HPMC E4M (% w/v)	0.5	0.5	0.5	0.5	0.5	0.5	0.5	0.5	0.5
Benzalkonium chloride (% w/v)	0.01	0.01	0.01	0.01	0.01	0.01	0.01	0.01	0.01
Mannitol (% w/v)	1.5	1.5	1.5	1.5	1.5	1.5	1.5	1.5	1.5
Disodium EDTA (% w/v)	0.05	0.05	0.05	0.05	0.05	0.05	0.05	0.05	0.05
STF q.s. to (mL)	10	10	10	10	10	10	10	10	10

STF: Simulated Tear Fluid; All formulations adjusted to pH 7.4 ± 0.1

Preparation of Puerarin-Loaded Ion-Triggered In Situ Gel

In situ gels loaded with puerarin were produced via a cooling process; hydration of gellan gum and xyloglucan from tamarind seeds occurred overnight at 4°C in STF buffer having a pH of 7.4. This allowed for complete swelling of polymers. Hydrodispersion of HPMC followed heating to 80°C and subsequent cooling. Precise amounts of puerarin (10 mg per ten millilitres) were dissolved in an amount of propylene glycol sufficient to produce a clear solution. Polymer blends were subsequently mixed continuously under stirring at 500 rpm at 25°C. Continuous stirring enabled incorporation of the resulting drug solution into these polymer blends. Addition of mannitol served to adjust tonicity whereas sodium disoxime acted as a penetration enhancer along with addition of benzalkonium chloride (0.01% weight/volume) as a preservative. Formulations were finally adjusted to volume of 10 mL with STF and pH was adjusted to 7.4 ± 0.1 utilizing 0.1N NaOH or hydrochloric acid under sterile conditions and filtered through membranes with pores of 0.22 μm.

Characterization of Formulations

Visual Appearance and pH

Visual inspection was performed on all formulations regarding clarity, coloration and the presence of particles. pH values of each formulation were determined by means of a calibrated digital pH meter (Eutech Instruments model PC 700 from India) at 25°C (n = 3); acceptable range of pH is between 6.5 and 7.8 to assure suitability for ocular compatibility [31, 32].

Viscosity

Viscosity of solid state formulations prior to gel formation were determined by means of Brookfield viscometer (DV II Plus model from Brookfield Engineering Ltd., USA), fitted with spindle S18 and operated at temperature 25°C and rotation speed 100 rpm for 60 s. Results were reported in units of mPa s (n = 3).

Gelation Temperature

The gelation temperature was determined by placing 2 mL of formulation into a vial that contained a thermometer. This vial underwent gradual heating within an aqueous bath (manufactured by Narang Scientific Works using model number NSW 143 from India), at a rate of 1°C per minute. Upon inversion of the vial the temperature at which the formulation stopped flowing is recorded as gelation temperature (n = 3).

Gel Strength

Gel strength was measured through immersion of 100 mL of formulation into solid tissue fluid at 37°C for 5 min so that complete gel formation could occur. Following immersion, 35 g were then placed upon the surface of the gel; penetration depth into the gel of 5 cm was subsequently recorded as measure of gel strength. Greater values indicate greater robustness of gel matrix (n = 3).

Drug Content

A precisely measured volume (one milliliter) of each formulation was dissolved in 10 mL of methanol by means of sonication for 15 min. Solution filtration then occurred via use of a membrane filter having pore size of 0.45 µm followed by appropriate dilution using standard test fluid before performing spectrophotometry at wavelength of 250 nm [33]. Content of drug substance was subsequently determined relative to calibration curve and expressed as percentage weight per volume; n equals three. Acceptability limits ranged from 98% up to 102% of claimed labeling claims.

Mucoadhesive Strength

Strength of mucoadhesion was assessed by means of a modification of texture analysis methodology. Fresh conjunctival membranes freshly excised from goats procured locally from slaughterhouse were affixed onto the lower probe. Gel formulation of 0.5 g was applied to an upper probe surface. Separation of probes occurred after 5 min of contact at 37°C under preload load of 0.5 N at a separation velocity of 0.5 mm/s utilizing texture analyser (Stable Micro Systems, TA XT plus, United Kingdom). Data for measured cohesive forces in dyn/cm² and adhesive work in joules is reported (n = 3).

In Vitro Drug Release

In vitro drug release experiments were conducted using Franz diffusion cells (manufactured by Permegear, United States) that included cellulose acetate membranes soaked for over one night with Substance T Fatty (STF) [34, 35]. Formulation material was placed into donor chamber containing 1 mL volume; receiver chamber contained 20 mL of STF solution pH 7.4 which was maintained at temperature of 35 ± 0.5°C and stirred continuously at rotation rate of 300 rpm. At predetermined times aliquots of 1 mL were drawn periodically and replaced with equal volumes of fresh STF. Sample analysis was carried out spectrophotometrically at wavelength of 250 nm. Cumulative percent drug release values were then calculated and plotted against time. Kinetic release profiles were assessed by fitting experimental data to zero order, first order, Higuchi model and also to Korsmeyer Peppas model and each comparison used triplicate samples [36, 37].

Ex Vivo Corneal Permeation Study

Ex vivo evaluation of corneal permeation utilized fresh excised corneas from goats which were placed in Franz diffusion cells such that the epithelium faced the donor compartment [38, 39]. Donor compartments received 1 mL of an optimized formulation and receptor compartments contained 20 mL of STF (pH 7.4) maintained at 35 ± 0.5°C and stirred at 300 rpm. Sample aliquots of 1 mL were withdrawn at one, two, four, 6 and 8 h and replaced with fresh

STF. Concentration of drug was measured spectrophotometrically at wavelength 250 nm. Calculation of apparent permeability coefficient Papp used the corresponding equation.

$$Papp = (dQ/dt) / (A \times C_0)$$

Where dQ by dt represents steady state flow rate (μg/s), A denotes diffusive surface area (square centimeters) and C sub 0 indicates initial concentration of donors (μg/mL); n equals three.

Isotonicity (Osmolality)

Measurement of osmolality of all formulations was performed utilizing a freezing point depression osmometer (Advanced Instruments model 3300; USA). Approximately 0.5 mL of each formulation were then placed in the sample cups and analyzed. The acceptable range of osmolality for ophthalmic formulations has been determined to be 280 to 320 mOsm per kg (n = 3).

Accelerated Stability Studies

Accelerated stability studies were conducted on an optimized batch according to ICH Q1A (R2) guidelines [40]. The composition was filled into vials that were sterile and amber colored and sealed; these were then stored at 40 ± 2°C and 75% relative humidity ± 5% relative humidity within a chamber (Thermost Lab Scientific Equipment Pvt. Ltd., Mumbai, India) for 6 months. At predesignated times of 0, 1, 3 and 6 months samples were removed and investigated for physical appearances, pH levels including gel pH level, gelling capability, viscosity both before and after gelling, drug content, release of drug at 12 h and muco adhesion strength. Evaluation methods are detailed in sections 2.7.1 through 2.7.6. Differences among time points were statistically significant determined by analysis of variance (ANOVA p greater than 0.05) using GraphPad Prism version 9.0 (n = 3) [41].

Results and Discussion

Calibration Curve of Puerarin

A calibration curve was constructed using purified puerarin in solution of sodium phosphate buffer at pH 7.4 at maximum absorbance wavelength of 250 nm and exhibited excellent linearity over the concentration range from 2 to 12 μg/mL and produced the regression equation y equals 0.0711 x plus 0.0042 with a coefficient of determination R^2 equaling 0.9993 (see Fig. 1). Results confirm suitability of the spectroscopic method thus far developed for precise quantitation of puerarin during further analysis.

Solubility Studies

Equilibrium solubility results for puerarin across different solvents are displayed in Table 3. Results show that aqueous solubility of puerarin increased markedly upon transition to physiological fluids, reaching 7.38 ± 0.28 mg/mL in STF at pH 7.4 and further increasing to 7.52 ± 0.31 mg/mL in PBS also at pH 7.4 and thus considered soluble. Dissolution results obtained from phosphate buffer solution at pH 6.8 were 4.16 ± 0.22 mg/mL demonstrating dependence on pH. Of organic solvents methanol exhibited highest solubility amounting to 38.64 ± 1.42 mg/mL whereas ethanol produced 24.18 ± 0.96 mg/mL which together justify selection of propylene glycol as preferred cosolvent during formulation development facilitating complete dissolution prior to incorporation into aqueous gel matrices.

Table 3
Equilibrium Solubility of Puerarin in Various Solvents at 25 ± 0.5°C

S. No.	Solvent	Solubility (mg/mL)	Classification
1	Distilled water	0.84 ± 0.06	Slightly Soluble
2	Simulated Tear Fluid (pH 7.4)	7.38 ± 0.28	Slightly Soluble
3	Phosphate Buffer Saline (pH 7.4)	7.52 ± 0.31	Slightly Soluble
4	Phosphate Buffer (pH 6.8)	4.16 ± 0.22	Slightly Soluble
5	Methanol	38.64 ± 1.42	Soluble
6	Ethanol	24.18 ± 0.96	Sparingly Soluble

All values Mean ± SD, n = 3

FTIR analysis

FTIR spectral analysis of pure puerarin (Fig. 2A) revealed characteristic absorption bands at 3374.41 cm^{-1} and 3273.74 cm^{-1} (O–H stretching of phenolic hydroxyl and glucosyl moieties), 3195.33 cm^{-1} (aromatic C–H stretch), 2920.70 and 2878.41 cm^{-1} (aliphatic C–H stretching), 1692.96 cm^{-1} (C = O stretching of isoflavone carbonyl), 1610.70 and 1586.55 cm^{-1} (aromatic C = C ring stretching), 1442.25 and 1389.94 cm^{-1} (C–H bending), 1265.18 cm^{-1} (C–O–C stretching of glycosidic linkage), 1031.62 and 960.58 cm^{-1} (C–O stretching), and fingerprint region peaks at 835.65,780.12,694.04, and 650.19 cm^{-1}. The physical mixture spectrum (Fig. 2B) retained all principal characteristic peaks of puerarin with minor positional shifts O–H stretching at 3433.42, 3396.21, 3340.83, and 3255.23 cm^{-1}; carbonyl C = O at 1631.86 cm^{-1}; aromatic C = C at 1610.31 and 1584.21 cm^{-1}; glycosidic C–O–C at 1034.57 cm^{-1}; and fingerprint peaks at 811.24,782.39,720.58, and 603.77 cm^{-1} with no significant peak disappearance or emergence of new bands, collectively confirming the absence of any physicochemical incompatibility between puerarin and the selected excipients.

Characterization of Puerarin-Loaded Ion-Triggered In Situ Gel

Visual Appearance and Gelling Capacity

Clear and colorless liquid formulations (F1 through F9) were present in solution form with total absence of particle matter, which confirms high levels of optical transparency appropriate for ophthalmic delivery as shown in Table 4. There is an increasing trend towards physical viscosity as concentration of polymers increases; formulation F1 through F4 remain fluid while F3, F5 and F7 appear slightly viscous and F6, F8 and F9 exhibit distinct viscosity as liquids. Contact with STF at pH 7.4 and temperature 34°C results in systematic improvement of gelling capacity ranging from soft transient gelation in formulation F1 marked by positive sign to strong persistent gels in F8 and F9 exhibiting ++++. It demonstrates that concomitant rise in concentration of both gellan gum and Tamarind Seed Xyloglucan strongly enhances the behavior of triggered solidification into gel and also prolongs persistence on simulated ocular surface.

Across all formulation gelation pH varied between 7.2 ± 0.04 and 7.4 ± 0.02 and is consistent with physiological tear fluid pH range thus demonstrating reproducible ion triggered gelation following instillation wherein there was no premature phase transition during storage as demonstrated in Table 5. Viscosity prior to gelation increased progressively from 42.3 ± 1.12 mPa·s for formulation F1 to 148.2 ± 2.96 m Pa s for formulation F9; however viscosity after introduction of standard tear fluid (STF) rose markedly from 684 ± 12.4 m Pa s to 3124 ± 38.7 m Pa s

which reflects concentration dependent cross linking ability by gellan gum ions with respect to tear fluid. Strength of gel ranged from 28.4 ± 0.82 sec for formulation F1 to 74.6 ± 1.63 sec for formulation F9 and mucosal adhesion strength ranged from 512.4 ± 6.21 dyn/cm² to 628.5 ± 8.96 dyn/cm² both of which increase with concentration indicating an enhanced potential for retention at precorneal site. Content of drug remains within 98.21 to 99.82% for all batches which falls well within acceptance criterion of 98 to 102%. Throughout osmolality levels remain within range of 280 to 320 milliosmoles per kilogram thereby confirming isotony of all formulations.

Table 4
Visual Appearance and Clarity of Puerarin-Loaded Ion-Triggered *In Situ* Gel Formulations (F1-F9)

Batch	Physical State (Sol)	Color	Clarity	Particulate Matter	Gelation upon Contact with STF
F1	Free-flowing liquid	Colorless	Clear	Absent	+
F2	Free-flowing liquid	Colorless	Clear	Absent	++
F3	Slightly viscous liquid	Colorless	Clear	Absent	++
F4	Free-flowing liquid	Colorless	Clear	Absent	++
F5	Slightly viscous liquid	Colorless	Clear	Absent	+++
F6	Viscous liquid	Colorless	Clear	Absent	+++
F7	Slightly viscous liquid	Colorless	Clear	Absent	+++
F8	Viscous liquid	Colorless	Clear	Absent	++++
F9	Viscous liquid	Colorless	Clear	Absent	++++

Scoring for Gel Formation: + corresponds to soft gels that dissolve within one to 2 h; ++ indicates moderately formed gels which persist from two to 4 h; +++ denotes firm gels that remain stable for four to 6 h; ++++ represents strong gels that maintain integrity beyond 6 h when contacted with STF at pH 7.4 and temperature of 34°C.

Table 5
Physicochemical Characterization of Puerarin-Loaded Ion-Triggered In Situ Gel Formulations F1–F9

Batch	Gelation pH *(Mean ± SD)*	Gelling Capacity (Score)	Viscosity Before Gelation (mPa·s)	Viscosity After Gelation with STF (mPa·s)	Gel Strength (sec)	Drug Content (%)	Mucoadhesive Strength (dynes/cm²)	Osmolality (mOsm/kg)
F1	7.2 ± 0.04	+	42.3 ± 1.12	684 ± 12.4	28.4 ± 0.82	98.21 ± 0.42	512.4 ± 6.21	284 ± 3.1
F2	7.2 ± 0.03	++	68.5 ± 1.54	1124 ± 18.6	38.6 ± 0.94	98.74 ± 0.38	524.6 ± 5.84	287 ± 2.8
F3	7.3 ± 0.03	++	98.7 ± 2.11	1842 ± 24.3	52.3 ± 1.21	99.12 ± 0.51	537.2 ± 7.12	291 ± 3.4
F4	7.2 ± 0.04	++	58.4 ± 1.34	986 ± 16.2	35.2 ± 0.76	98.56 ± 0.44	548.8 ± 6.54	289 ± 2.6
F5	7.3 ± 0.03	+++	86.2 ± 1.87	1648 ± 21.8	48.7 ± 1.08	99.34 ± 0.36	572.4 ± 5.97	293 ± 2.9
F6	7.3 ± 0.02	+++	124.6 ± 2.43	2486 ± 31.4	64.5 ± 1.45	99.68 ± 0.29	589.6 ± 8.23	298 ± 3.7
F7	7.3 ± 0.03	+++	76.8 ± 1.62	1386 ± 19.4	44.1 ± 0.98	98.89 ± 0.47	581.3 ± 6.78	294 ± 2.7
F8	7.4 ± 0.02	++++	108.3 ± 2.28	2184 ± 28.6	58.9 ± 1.32	99.41 ± 0.33	604.7 ± 7.45	301 ± 3.2
F9	7.4 ± 0.02	++++	148.2 ± 2.96	3124 ± 38.7	74.6 ± 1.63	99.82 ± 0.24	628.5 ± 8.96	307 ± 4.1

All values Mean ± SD, n = 3

Cumulative In Vitro Drug Release

Illustrated in Fig. 3 is the cumulative in vitro profile of drug release for formulations F1 to F9 during 12 h. Controlled and sustained drug release characteristics typical of ion responsive hydrogel matrices were observed consistently among all formulations; release declined progressively concomitant with rising concentration levels of polymers. Release from formulation F1 exceeded that of others by 97.28% after 12 h whereas F9 exhibited the least release amounting to 73.86% after this time period due to formation of denser networks resulting from increasing concentrations of gellan gum and xyloglucan derived from tamarind seeds. Batch F8 which was optimized released 82.42% of the cumulative drug load after 12 h satisfying target level of ≥ 80% thereby indicating appropriate balance between retention of gel integrity and sufficient drug permeability through depot gel.

Release Kinetics analysis

Kinetic modeling of an optimized batch F8 released demonstrated highest linearity using the Korsmeyer–Peppas model (R^2 value equaling 0.9995), second highest using Hixon Crowell (R^2 value equaling 0.9972) and third highest according to zero order (R^2 value equaling 0.9865) as shown in Fig. 4. Diffusion exponent n assessed based on the Korsmeyer Peppas model equaled 0.7815 which falls within the range of 0.5 to 1 indicating that dominant release mechanism is anomalous rather than Fickian transport from the gel matrix.

Ex Vivo Corneal Permeation study

The *ex vivo* corneal permeation profiles of puerarin-loaded ion-triggered *in situ* gel formulations (F1–F9), evaluated across freshly excised goat cornea, are illustrated in Fig. 5. All formulations exhibited a time-dependent increase in cumulative drug permeation over the study period, with the permeation rate and extent varying appreciably across the batches. The steady-state flux (J) and apparent permeability coefficient (Papp) values, summarized in Table 6, ranged from 5.18 ± 0.14 to 8.24 ± 0.22 μg/cm²/h and 0.518 ± 0.014 × 10^{-3} to 0.824 ± 0.022 × 10^{-3} cm/h, respectively. Among the tested formulations, F9 demonstrated the highest permeation efficiency (J = 8.24 ± 0.22 μg/cm²/h; Papp = 0.824 ± 0.022 × 10^{-3} cm/h), followed by F6 (J = 7.84 ± 0.21 μg/cm²/h) and F8 (J = 7.68 ± 0.20 μg/cm²/h), whereas F1 showed the lowest permeation (J = 5.18 ± 0.14 μg/cm²/h). This progressive enhancement in flux and permeability across the formulation series suggests that the compositional variations among F1–F9 favorably modulated the interaction of the *in situ* gel matrix with the corneal barrier, facilitating improved transcorneal diffusion of puerarin. The consistently low standard deviations (n = 3) across all batches further indicate good reproducibility of the permeation behavior. Collectively, these findings suggest that the optimized ion-triggered *in situ* gel system enhances corneal permeability of puerarin, supporting its potential as an effective platform for sustained ocular drug delivery.

Table 6
Steady-State Flux (J) and Apparent Permeability Coefficient (Papp) of Puerarin-Loaded Ion-Triggered *In Situ* Gel Formulations F1–F9 Derived from Ex Vivo Corneal Permeation Study

Batch	Steady-State Flux, J (μg/cm²/h)	Papp × 10^{-3} (cm/h)
F1	5.18 ± 0.14	0.518 ± 0.014
F2	5.96 ± 0.16	0.596 ± 0.016
F3	6.84 ± 0.18	0.684 ± 0.018
F4	6.32 ± 0.17	0.632 ± 0.017
F5	7.16 ± 0.19	0.716 ± 0.019
F6	7.84 ± 0.21	0.784 ± 0.021
F7	6.94 ± 0.18	0.694 ± 0.018
F8	7.68 ± 0.20	0.768 ± 0.020
F9	8.24 ± 0.22	0.824 ± 0.022

All values Mean ± SD, n = 3

Optimization of Puerarin-Loaded Ion-Triggered In Situ Gel

Influence of Gellan Gum and Tamarind Seed Xyloglucan Concentrations on Gelation pH (Y_1)

Table 7 presents a concise summary which identifies linear model as being most suitable for description of gelation pH response (Y_1); it is supported by sequential p value of 0.0032 and an adjusted R^2 of 0.803 which indicates adequate explanation of 80.3% of variation of Y_1 through the linear model. Neither second factorial interaction nor quadratic models have been selected since their sequential p values (both 1.0000 and 0.4827 respectively) are not

significant at statistical level and offer no meaningful enhancement in terms of fitting quality. Results of analysis of variance summarised in Table 8 confirm general significance of the overall model (F value equals to 17.31 and p equals to 0.0032). Both independent variables display significant linear effect upon Y_1: gellan gum (A; F value equals 12.46 and p equals 0.0124) and tamarind seed xyloglucan (B; F value equals 22.15 and p equals 0.0033). Contribution of variable B stands out relative to other contributions to response to gelation pH.

Y_1 (GP) = + 7.289 + 0.05A + 0.06667B

Polynomial equation for Y_1 yielded positive coefficients for both independent variables A and B, indicating that increasing concentrations of each of guar gum and seeds of Tamarindus indica separately raised gelation pH towards upper limits within physiological tear fluid pH range which is 7.2 to 7.4. Coefficient value of variable B was slightly higher than that of A and thus confirmed slightly greater effect of seeds of Tamarindus indica upon gelation pH. Contour plots in two dimensions (Fig. 6A) display diagonal lines running parallel to one another and an upward progression of Y_1 values from the lower left to the upper right region of experimental design space which reflects additive linear relationship among both variables and gelation pH. Response surface plot in three dimensions (Fig. 6B) supports this finding by showing flat uncurved surfaces consistent with absence of significant quadratic or interaction terms selected in chosen linear model.

Influence of Gellan Gum and Tamarind Seed Xyloglucan Concentrations on Mucoadhesive Strength (Y_2)

Table 7 identifies 2 FI model as suggested model for muco adhesion strength (Y_2) and demonstrates good fit evidenced by low p value of 0.0339 along with high adjusted R^2 value at 0.990 which indicates that 99.0% of total variation in Y_2 is explained by the model. Linear model although significant (p less than 0.0001 and adjusted R^2 equals 0.9777) is surpassed because of significant contribution of interaction term AB (p equals 0.0339). Results from ANOVA summarized in Table 8 confirm significance of overall 2 FI model (F equals 264.86 and p less than 0.0001). Among separate factors tamarind seed xyloglucon B stands out as dominant (F equals 644.23 and p less than 0.0001) followed by gellan gum A (F equals 141.96 and p less than 0.0001); interaction term AB also shows statistical significance (F equals 8.397 and p equals 0.0339).

Y_2 (MS) = + 566.61 + 18.80A + 40.05B + 5.60AB

Coefficients were found for the polynomial equation of Y_2 demonstrating positive values for variable A + 18.80, variable B + 40.05 and interaction term AB + 5.60 which confirmed synergistic augmentation of mucoadhesion strength by both independent variables and their interaction. Quantitative comparison showed significantly greater coefficient of B compared to A (40.05 versus 18.80). This difference highlights xyloglucan derived from tamarind seeds as principal determinant of adhesion force because of their stronger binding affinity due to hydrogen bonds and physical entanglements. Positive value of the interaction coefficient indicates that combination of high concentrations of both polymers results in an additive enhancement of adhesion exceeding the sum of individual contributions. Contour plots (Fig. 6C) display curves trending towards higher Y_2 values with simultaneous increase of both concentration levels of A and B; steep gradients were noted along the axis of B. Three dimensional surface response plot (Fig. 6D) shows a uniformly ascending curved surface rising steeply from bottom left region corresponding to low concentration levels of A and B up to top right area characterized by high concentrations of both. Visually these confirm strong and synergistic contributions of both independent factors to adhesion strength.

Influence of Gellan Gum and Tamarind Seed Xyloglucan Concentrations on Ex Vivo Corneal Permeation at 8h (Y_3)

Table 7 specifies that the quadratic model is chosen as the best fitting one for extracorporeal permeability at 8 h (Y_3); it demonstrates significance via sequential p value at 0.0051 along with an adjusted R^2 value of 0.9989 which indicates that 99.89% of the total variance of Y_3 is accounted for by said model; this represents highest predictive performance among those three responses. Linear model shows significance at p less than 0.0001 but is inadequate. Improvement through 2FI model does not reach statistical significance (p equals 0.4121) thus requiring quadratic model to sufficiently capture nonlinear response behavior. Results reported in Table 8 confirm high significance of overall quadratic model (ANOVA; F equals 1397.63; p less than 0.0001). Amongst all terms tamarind seed xyloglucan (B) stands out as the single most influential factor (ANOVA; F equals 3654.63; p less than 0.0001) followed very closely by gellan gum (A; F equals 3219.22; p less than 0.0001). Interaction term AB (ANOVA; F equals 16.18; p equals 0.0276) and quadratic term B^2 (ANOVA; F equals 96.55; p equals 0.0022) show statistical significance whereas A^2 is not significant (ANOVA; F equals 1.586; p equals 0.2970).

$$Y_3\ (EVCP\%) = +64.48 + 7.89A + 8.407B + 0.685AB + 0.3033A^2 - 2.367B^2$$

Polynomial equations for Y_3 showed large positive linear coefficients for both A (with + 7.89) and B (with + 8.407). This indicates significant enhancement of cumulative permeation through cornea over 8 h due to substantial increase in concentrations of both gellan gum and xyloglucan from seeds of tamarind. Interaction coefficient also showed a modest synergy among A and B regarding permeability. Negative quadratic coefficient for B^2 (− 2.367) signified nonlinear responses where further increases of xyloglucan exceeded optimum concentrations led to attenuation of permeability because of formation of excessive adhesive mucilage network thereby inhibiting diffusion of drug. Coefficient A^2 (positive value + 0.3033) indicated that influence of gellan gum remained essentially linear within the study limits. Contour plots in two dimensions (Fig. 6E) display ellipses with peak Y_3 scores clustering in high levels of A and moderate to high levels of B but showing slight curvature along the B axis which reflects quadratic effects of xyloglucan clearly. Response surface plots in three dimensions (Fig. 6F) show an upwardly curved surface attaining a broad plateau at intermediate to higher concentrations of both polymers; however, there is a marginal decline at highest level of B concentration and this is consistent with negative coefficient B^2 and visual confirmation of optimal formulation space occupied by Batch F8 clearly.

Table 7
Fit Summary for Gelation pH (Y_1) and Mucoadhesive Strength (Y_2) and Ex Vivo Corneal Permeation at 8h (Y_3)

Source	Sequential p-value	Lack of Fit p-value	Adjusted R^2	Remark
Response 1: Gelation pH (Y_1)				
Linear	0.0032	-	0.803	Suggested
2FI	1.0000	-	0.7636	-
Quadratic	0.4827	-	0.7576	-
Cubic	0.5000	-	0.8182	Aliased
Response 2: Mucoadhesive Strength (Y_2)				
Linear	< 0.0001	-	0.9777	-
2FI	0.0339	-	0.99	Suggested
Quadratic	0.0711	-	0.9971	-
Cubic	0.6331	-	0.9966	Aliased
Response 3: Ex Vivo Corneal Permeation at 8h (Y_3)				
Linear	< 0.0001	-	0.9776	-
2FI	0.4121	-	0.9769	-
Quadratic	0.0051	-	0.9989	Suggested
Cubic	0.9548	-	0.9969	Aliased

Table 8
ANOVA Summary for the Linear / 2FI / Quadratic Model - Gelation pH (Y_1) and Mucoadhesive Strength (Y_2) and Ex Vivo Corneal Permeation at 8h (Y_3)

Source	Sum of Squares	df	Mean Square	F-value	p-value	Significance
Response 1: Gelation pH (Y_1)						
Model	**0.04167**	**2**	**0.02083**	**17.31**	**0.0032**	**Significant**
A - Gellan Gum	0.015	1	0.015	12.46	0.0124	Significant
B - Tamarind Seed Xyloglucan	0.02667	1	0.02667	22.15	0.0033	Significant
Residual	**0.007222**	**6**	**0.001204**	**-**	**-**	**-**
Cor Total	**0.04889**	**8**	**-**	**-**	**-**	**-**
Response 2: Mucoadhesive Strength (Y_2)						
Model	**11870.10**	**3**	**3956.70**	**264.86**	**< 0.0001**	**Significant**
A - Gellan Gum	2120.64	1	2120.64	141.96	< 0.0001	Significant
B - Tamarind Seed Xyloglucan	9624.01	1	9624.01	644.23	< 0.0001	Significant
AB	125.44	1	125.44	8.397	0.0339	Significant
Residual	**74.69**	**5**	**14.94**	**-**	**-**	**-**
Cor Total	**11944.79**	**8**	**-**	**-**	**-**	**-**
Response 3: Ex Vivo Corneal Permeation at 8h (Y_3)						
Model	**810.81**	**5**	**162.16**	**1397.63**	**< 0.0001**	**Significant**
A - Gellan Gum	373.51	1	373.51	3219.22	< 0.0001	Significant
B - Tamarind Seed Xyloglucan	424.03	1	424.03	3654.63	< 0.0001	Significant
AB	1.877	1	1.877	16.18	0.0276	Significant
A^2	0.184	1	0.184	1.586	0.2970	Not Significant
B^2	11.20	1	11.20	96.55	0.0022	Significant
Residual	**0.3481**	**3**	**0.116**	**-**	**-**	**-**
Cor Total	**811.16**	**8**	**-**	**-**	**-**	**-**

Validation of statistical model

Optimization run 8 was utilized for assessment of models against an actual batch. Gelatinization pH prediction was 7.356 and measurement obtained as 7.40; relative error was 0.6042%; Muco Adhesion strength prediction was

606.66 and measurement 604.70; permeation ex vivo at 8h prediction was 70.52 and measurement 70.24; relative error being 0.4033%. Overall desirability of the selected solution was 0.920. Deviations remain within acceptance limits of 5% and support predictive capability of fitted polynomials over studied design space. Full comparison is detailed in Table 9 entitled Validation Comparison of Predicted versus Actual Response Values.

Table 9
Validation of the optimized formulation (Run 8) - predicted vs. actual response values

Parameter	Factor A: Gellan Gum (% w/v)	Factor B: Tamarind Seed Xyloglucan (% w/v)	Y_1: Gelation pH	Y_2: Mucoadhesive Strength (dynes/cm²)	Y_3: Ex Vivo Corneal Permeation at 8h (%)	Desirability
Predicted Value	0.50	0.30	7.356	606.66	70.52	0.920
Actual Value (Run 8)	0.50	0.30	7.40	604.70	70.24	-
Absolute Error	-	-	0.04444	1.961	0.2844	-
Relative Error (%)	-	-	0.6042	0.3233	0.4033	-

Accelerated Stability study

Accelerated stability data for optimized batch F8 which was stored at 40 ± 2°C and relative humidity levels ranging between 75 ± 5% for six months is presented in Table 10. Throughout the duration of this study each parameter that has been assessed consistently remains within predefined acceptance criteria showing little variation. There is no discernible change noted in physical appearance, retention of gel forming capacity (+++ maintained continuously through different intervals), gel formation pH ranging from 7.4 to 7.3 and also formulation pH also ranging from 7.4 to 7.3. Content of active pharmaceutical ingredient declines slightly from 99.41 ± 0.33% units to 98.84 ± 0.42% units; degree of release decreases from 82.42 ± one point three four percentage units to 81.54 ± one point four six percentage units; muco adhesion strength falls from 604.7 ± seven point forty five dyn/cm² to 600.4 ± seven point eighty six dyn/cm² and osmotic pressure rises from 301 ± three point two mOsmoles per kilogram to 303 ± three point eight mOsmoles per kilogram. Within specification limits these values remain stable. No statistically significant differences were observed among various time points according to results of analysis of variance conducted on one way basis (p greater than 0.05). This confirms robustness of physical chemistry characteristics of F8 under stress storage conditions.

Table 10
Accelerated Stability Data of Optimized Batch F8 at 40 ± 2°C / 75% RH ± 5% RH for Six Months.

Parameter	Initial (0 Month)	1 Month	3 Months	6 Months
Physical Appearance	Clear, Colorless, free-flowing	Clear, colorless, free-flowing	Clear, colorless, free-flowing	Clear, colorless, free-flowing
pH	7.4 ± 0.02	7.4 ± 0.02	7.3 ± 0.03	7.3 ± 0.03
Gelation pH	7.4 ± 0.02	7.4 ± 0.02	7.4 ± 0.02	7.3 ± 0.03
Gelling Capacity	++++	++++	++++	++++
Viscosity Before Gelation (mPa·s)	108.3 ± 2.28	109.1 ± 2.34	110.4 ± 2.41	111.2 ± 2.48
Viscosity After Gelation (mPa·s)	2184 ± 28.6	2196 ± 29.4	2208 ± 30.1	2221 ± 31.2
Drug Content (%)	99.41 ± 0.33	99.28 ± 0.36	99.06 ± 0.38	98.84 ± 0.42
Osmolality (mOsm/kg)	301 ± 3.2	302 ± 3.4	302 ± 3.6	303 ± 3.8
Drug Release at 12h (%)	82.42 ± 1.34	82.18 ± 1.38	81.86 ± 1.42	81.54 ± 1.46
Mucoadhesive Strength (dynes/cm²)	604.7 ± 7.45	603.2 ± 7.62	601.8 ± 7.74	600.4 ± 7.86

All values Mean ± SD, n = 3

Discussion

Analytical results along with preliminary formulation work provided an adequate basis for further development of gels based on loading puerarin by means of ion triggering in situ [42]. Calibration curves built using standard solution at λmax 250 nm in STF (pH 7.4) revealed high linearity (R^2 equal to 0.9993; see Fig. 1). Results conformed well with previously reported methods utilizing similar wavelengths for quantitation of puerarin and thus validate the developed analytical procedure for subsequent estimation of drug content [43]. Results from solubility studies summarized in Table 3 indicated that puerarin has low solubility in aqueous phase and recorded values of 0.84 ± 0.06 mg/mL in distilled water. Values improved significantly to 7.38 ± 0.28 mg/mL in STF (pH 7.4) indicating suitability of such physiological environment for dissolution and permeation studies [44]. Higher solubility was observed also in methanol (mean value 38.64 ± 1.42 mg/mL) and ethanol (mean value 24.18 ± 0.96 mg/mL) suggesting that propylene glycol should be chosen as cosolvent during formulating process [45]. Fourier transform infrared spectroscopy (FTIR) data presented in Fig. 2 confirmed retention of characteristic peaks of puerarin including carbonyls at 1692.96 cm^{-1} one and glycosidic C O C stretching vibrations at 1265.18 cm^{-1} one [46]. No appearance of additional bands suggested absence of compatibility between drug and excipients which is necessary prior to proceeding towards developing formulations [47].

Physicochemical characterization was performed on all nine formulations (Tables 4 and 5) [48]. Results indicated that combined concentrations of guar gum and seeds of Tamarindus indica xylan were responsible for key quality attributes of the self triggered in situ gel system [49]. Values of gel formation pH ranged from 7.2 to 7.4 among formulations F1 to F9 and confirm that the gel phase transitions reliably occur within physiological tear fluid pH range; this is a crucial prerequisite for activated ionic ocular systems [50]. Progressive increases in viscosity after

gel formation (684 to 3124 mPa·s), gel strength (28.4 to 74.6 sec) and muco adhesion strength (512.4 to 628.5 dyn/cm²) correlated consistently with well established mechanism involving cations such as sodium, potassium and calcium ions binding at sites of negative charges on the backbone of guar gum and subsequent formation of a denser three dimensional network. Superior performance in terms of muco adhesion noted for high concentration batches is due to known affinity of seeds of Tamarindus indica xylan towards mucins mediated via hydrogen bonding with mucin glycoproteins, a feature which has not been exploited before in systems based on triggered ionic gelation for ocular applications and represents a new contribution of this study. Content of drug substance (98.21 to 99.82%) and osmotic pressure (284 to 307 milliosmoles per kilogram) conform uniformly to accepted standards and specifications across all batches.

Analysis based upon a 3² factorial design determined statistically significant effects dependent on concentration levels of two independent variables on each of three response variables [51]. Results from Table 7 and Table 8 indicate that gelation pH (Y_1) has linear models which fit adequately (adjusted R^2 value is 0.803); B, derived from Tamarind Seed Xyloglucan (B; F ratio equals 22.15, P value is 0.0033) exhibits greater influence compared to Gellan Gum A (F ratio equal to 12.46, P value is 0.0124) [52]. Muco Adhesion Strength (Y_2) is better modeled by second order Factor Interaction (FI) model (adjusted R^2 value is 0.990), AB showing synergy (F ratio equals 8.397, P value is 0.0339) with B being predominant factor (F ratio equals 644.23, P value less than 0.0001), consistent with high contribution of Tamarind Seed Xyloglucan. Ex vivo Corneal Permeation at 8h (Y_3) shows identification of significant quadratic negative effect of B (B^2; F ratio equals 96.55, P value equals 0.0022) suggesting higher concentrations of xyloglucan lead to formation of excessively tight mucoadhesive barriers and thereby reducing permeation [53]. Response surface plots display clear evidence of such nonlinearity [54]. Batch F8, optimized using concentrations of 0.5% weight per volume of Gellan Gum and 0.3% weight per volume of Tamarind Seed Xyloglucan meets validation criteria with predicted values differing from actual ones by less than 1% for all responses (Table 9, overall desirability equals 0.920). Predicted values of diffusion exponent n (value equals 0.7815, R^2 equals 0.9995) for F8 suggest anomalous non Fickian transport indicative of combined diffusion through swollen gel matrices and relaxation of polymer chains – release profile typical of muco adhesive hydrogel ocular systems and favorable for prolonged precorneal drug delivery management of dry eye disease [55].

Acceleration of accelerated stability studies performed at 40 ± 2°C and relative humidity at 75 ± 5% for six months demonstrated excellent physical chemical stability, with retention of all parameters within acceptance criteria and lack of statistically significant variations among different sampling times (ANOVA one way, p greater than 0.05) [56]. This projection suggests a shelf life exceeding 2 year according to ICH Q1 A R2 guidelines. Steady state flux (J equal 7.68 ± 0.20 µg/cm² per hour) and apparent permeability coefficient (Papp equals 0.768 times ten to the negative third power cm/h) of F8 (see Table 6) was markedly higher compared to lower concentration formulations and thus affirmed effective prolongation of corneal contact time together with facilitating sustained transcorneal penetration of puerarin [57]. Limitations of the current investigation merit consideration: excised corneal permeation used goats corneas as surrogates which does not fully reproduce human corneal barrier characteristics; in vivo pharmacokinetic and pharmacodynamic validations using appropriate models of dry eye disease have yet to be conducted; and further clinical evaluations regarding longer ocular tolerance beyond assessment by HET CAM are required before translation [58].

Conclusion

This study successfully developed and optimized an injectable gel based on loading with puerarin for ocular delivery suitable for patients suffering from dry eye disease through application of a three by two factorial

experimental design. Gelatin gum and xyloglucan derived from Tamarind seeds serve as principal ionsensitive gelling agents and new mucolytic adhesives, respectively. Batch F8 which contains 0.5% weight volume of gelatin gum and 0.3% weight volume of xyloglucan derived from seeds of Tamarind exhibited physiologically appropriate gel formation at pH 7.4 ± 0.02, strong gel forming ability (++++), high muco affinity strengths reaching 604.7 ± 7.45 dyn/cm², sustained release greater than 80% after 12 h and permeability flux (Papp) of 0.768 times ten to negative third cm/h; together these results confirm that the formulation overcomes intrinsic deficiencies associated with conventional eye drops such as fast clearance from precorneal site and insufficient drug concentration at ocular surface level. Further support for pharmaceutical robustness and translational clinical potential is provided by anomalous non-Fickian release behavior along with good accelerated stability results lasting six months. Promising results thus suggest advancement towards subsequent studies involving pharmacokinetics, pharmacodynamics and ocular tolerance evaluation in proper animal models of dry eye disease to definitively assess efficacy and safety before undertaking clinical development.

Abbreviations

ANOVA
Analysis of Variance
BP
British Pharmacopoeia
BCS
Biopharmaceutics Classification System
CDXML
ChemDraw XML
CZE
Capillary Zone Electrophoresis
DED
Dry Eye Disease
DSC
Differential Scanning Calorimetry
EDTA
Ethylenediaminetetraacetic Acid
EVCP
Ex Vivo Corneal Permeation
2FI
Two-Factor Interaction
FTIR
Fourier-Transform Infrared Spectroscopy
GP
Gelation pH
HET-CAM
Hen's Egg Test on Chorioallantoic Membrane
HPMC
Hydroxypropyl Methylcellulose
ICH
International Council for Harmonisation

IP
Indian Pharmacopoeia
J
Steady-State Flux
KBr
Potassium Bromide
LOD
Limit of Detection
LOQ
Limit of Quantification
MS
Mucoadhesive Strength
MW
Molecular Weight
NIR
Near-Infrared Spectroscopy
Papp
Apparent Permeability Coefficient
PBS
Phosphate Buffer Saline
pH
Potential of Hydrogen
PUE
Puerarin
R^2
Correlation Coefficient
RH
Relative Humidity
RP-HPLC
Reversed-Phase High-Performance Liquid Chromatography
SD
Standard Deviation
STF
Simulated Tear Fluid
TLC
Thin-Layer Chromatography
USP
United States Pharmacopoeia
UV
Ultraviolet Spectroscopy
v/v
Volume by Volume
w/v
Weight by Volume

λmax
Wavelength of Maximum Absorbance.

Declarations

Acknowledgements

Authors express sincere thanks to principal of institute for provision of requisite laboratory infrastructure and instrumental facilities along with academic support which was essential for successful accomplishment of research work herein. Authors likewise acknowledge graciously Quaestive Innovation Private Limited of Pune, India for generous supply of required reagents and plant extracts together with continuous technical support throughout the course of study. Contributions from all laboratory personnel and research associates who cooperated in development of formulations and performance of analytical studies are also greatly esteemed profoundly.

Authors' Contribution

All authors contributed equally.

Funding Declaration

Not applicable

Ethics declaration

Not applicable

Conflict of Interest

The authors declare no conflict of interest.

References

1. López-Machado, A., Díaz-Garrido, N., Cano, A., Espina, M., Badia, J., Baldomà, L., … Sánchez-López, E. (2021). Development of Lactoferrin-Loaded Liposomes for the Management of Dry Eye Disease and Ocular Inflammation. *Pharmaceutics*, *13*(10), 1698. https://doi.org/10.3390/pharmaceutics13101698
2. Li, B., & Kang, Y. (2026). Paget's disease of bone: pathogenesis, ocular manifestations, and therapeutic strategies. *Orphanet Journal of Rare Diseases*, *21*(1). https://doi.org/10.1186/s13023-026-04412-4
3. Shukla, A. K., Bishnoi, R. S., Kumar, M., Fenin, V., & Jain, C. P. (2018). Applications of Tamarind seeds Polysaccharide-based copolymers in Controlled Drug Delivery: An overview. *Asian Journal of Pharmacy and Pharmacology*, *4*(1), 23–30. https://doi.org/10.31024/ajpp.2018.4.1.5
4. Alotaibi, W., Abusharha, A., Pearce, E., Althomali, M., Afsar, T., & Razak, S. (2024). Assessment of Tamarind Seed Polysaccharide (TSP) and Hyaluronic Acid (HA) Containing Ophthalmic Solution to Maintain Tear Osmolarity, Ocular Surface Temperature (OST) and Tear Production. *Clinical Ophthalmology*, *Volume 18*, 3503–3513. https://doi.org/10.2147/opth.s493336
5. Lee, H., Jeon, S., Kim, C. E., Park, Y.-J., & Yang, J. (2019). A New Ophthalmic Pharmaceutical Formulation, Topical Sulglycotide, Enhances the Ocular Mucin Secretion in Desiccation Stress-Mediated Dry Eye Disease. *Investigative Opthalmology & Visual Science*, *60*(4), 1076. https://doi.org/10.1167/iovs.18-24935

6. Yang, J., Tan, H., Peng, X., & Nie, S. (2025). Tamarind Seed-Derived Xyloglucan Attenuates Insulin Resistance in Mice through Gut Microbiota. *Journal of Agricultural and Food Chemistry*, *73*(47), 30236–30256. https://doi.org/10.1021/acs.jafc.5c07829
7. Jiang, K., Wang, D., Su, L., Liu, X., Yue, Q., Zhang, S., & Zhao, L. (2023). Tamarind Seed Polysaccharide Hydrolysate Ameliorates Dextran Sulfate Sodium-Induced Ulcerative Colitis via Regulating the Gut Microbiota. *Pharmaceuticals*, *16*(8), 1133. https://doi.org/10.3390/ph16081133
8. Chen, Y., Li, X., Sun, X., Kou, Y., Ma, X., Song, L., … Wu, Y. (2025). Joint transcriptomics and metabolomics unveil the protective mechanism of tamarind seed polysaccharide against antibiotic-induced intestinal barrier damage. *International Journal of Biological Macromolecules*, *305*(Pt 1), 140999. https://doi.org/10.1016/j.ijbiomac.2025.140999
9. Ghenciu, L. A., Andrei, D., Borza, C., Iacob, R., Stoicescu, E. R., Bolintineanu, S. L., … Haţegan, O. A. (2025). Therapeutic Potential of Rho Kinase Inhibitors in Corneal Disease: A Systematic Review of Preclinical and Clinical Studies. *Biomedicines*, *13*(7), 1602. https://doi.org/10.3390/biomedicines13071602
10. Gong, D., Chen, H., Wang, H., Witman, N., Lu, Y., Fu, Y., & Fu, W. (2026). M2 macrophage-derived exosomes deliver NGF-modified mRNA to promote comprehensive corneal repair. *Journal of Controlled Release*, *395*, 114930. https://doi.org/10.1016/j.jconrel.2026.114930
11. Zou, H., Hong, Y., Xu, B., Wang, M., Xie, H., & Lin, Q. (2024). Multifunctional cerium oxide nanozymes with high ocular surface retention for dry eye disease treatment achieved by restoring redox balance. *Acta Biomaterialia*, *185*, 441–455. https://doi.org/10.1016/j.actbio.2024.07.003
12. Li, X., Kang, B., Woo, I. H., Eom, Y., Lee, H. K., Kim, H. M., & Song, J. S. (2018). Effects of Topical Mucolytic Agents on the Tears and Ocular Surface: A Plausible Animal Model of Mucin-Deficient Dry Eye. *Investigative Opthalmology & Visual Science*, *59*(7), 3104. https://doi.org/10.1167/iovs.18-23860
13. Inam, M., Liu, L., Wang, J.-W., Yu, K.-X., Phan, C.-U., Shen, J., … Hu, X. (2021). Enhancing the Physiochemical Properties of Puerarin via L-Proline Co-Crystallization: Synthesis, Characterization, and Dissolution Studies of Two Phases of Pharmaceutical Co-Crystals. *International Journal of Molecular Sciences*, *22*(2), 928. https://doi.org/10.3390/ijms22020928
14. Park, J., Park, J. E., Hedrick, V. E., Wood, K. V., Bonham, C., Lee, W., & Yeo, Y. (2018). A Comparative In Vivo Study of Albumin-Coated Paclitaxel Nanocrystals and Abraxane. *Small*, *14*(16), e1703670. https://doi.org/10.1002/smll.201703670
15. Ahmed, S., Amin, M. M., & Sayed, S. (2023). Ocular Drug Delivery: a Comprehensive Review. *AAPS PharmSciTech*, *24*(2), 66. https://doi.org/10.1208/s12249-023-02516-9
16. Wang, Y., & Wang, C. (2022). Novel Eye Drop Delivery Systems: Advance on Formulation Design Strategies Targeting Anterior and Posterior Segments of the Eye. *Pharmaceutics*, *14*(6), 1150. https://doi.org/10.3390/pharmaceutics14061150
17. Raj, V., & Lee, S. (2024). State-of-the-art progress on tamarind seed polysaccharide (Tamarindus indica) and its diverse potential applications, a review with insight. *Carbohydrate Polymers*, *331*, 121847. https://doi.org/10.1016/j.carbpol.2024.121847
18. Manna, S., Sarkar, S., Paul, P., Sahu, R., Dua, T. K., & Nandi, G. (2025). Drug delivery and biomedical applications of tamarind seed xyloglucan and its derivatives: a review. *Journal of Biomaterials Science, Polymer Edition*, 1–37. https://doi.org/10.1080/09205063.2025.2582700
19. Ghaee, A., Karimi, M., Lotfi-Sarvestani, M., Sadatnia, B., & Hoseinpour, V. (2019). Preparation of hydrophilic polycaprolactone/modified ZIF-8 nanofibers as a wound dressing using hydrophilic surface modifying

macromolecules. *Materials Science and Engineering: C*, *103*, 109767. https://doi.org/10.1016/j.msec.2019.109767

20. Lee, J.-H., Jo, J.-K., Kim, D.-A., Patel, K. D., Kim, H.-W., & Lee, H.-H. (2018). Nano-graphene oxide incorporated into PMMA resin to prevent microbial adhesion. *Dental Materials*, *34*(4), e63–e72. https://doi.org/10.1016/j.dental.2018.01.019
21. Hu, L., Xu, Y., & Meng, H. (2022). Development and Evaluation of Puerarin Loaded-Albumin Nanoparticles Thermoresponsive in situ Gel for Ophthalmic Delivery. *Drug Design, Development and Therapy*, *Volume 16*, 3315–3326. https://doi.org/10.2147/dddt.s374061
22. Zaid Alkilani, A., Hamed, R., Abdo, H., Swellmeen, L., Basheer, H. A., Wahdan, W., & Abu Kwiak, A. D. (2022). Formulation and Evaluation of Azithromycin-Loaded Niosomal Gel: Optimization, In Vitro Studies, Rheological Characterization, and Cytotoxicity Study. *ACS Omega*, *7*(44), 39782–39793. https://doi.org/10.1021/acsomega.2c03762
23. Phumkacha, A., Leejarkpai, T., Cheutor, S., Sriariyanun, M., & Kirdponpattara, S. (2025). Development of Tamarind Seed Polysaccharide-Derived Edible Films for Postharvest Grape Preservation. *Journal of Food Science*, *90*(6), e70312. https://doi.org/10.1111/1750-3841.70312
24. Jha, S., Malviya, R., Fuloria, S., Sundram, S., Subramaniyan, V., Sekar, M., … Fuloria, N. K. (2022). Characterization of Microwave-Controlled Polyacrylamide Graft Copolymer of Tamarind Seed Polysaccharide. *Polymers*, *14*(5), 1037. https://doi.org/10.3390/polym14051037
25. Dalvi, A., Ravi, P. R., & Uppuluri, C. T. (2021). Rufinamide-Loaded Chitosan Nanoparticles in Xyloglucan-Based Thermoresponsive In Situ Gel for Direct Nose to Brain Delivery. *Frontiers in Pharmacology*, *12*, 691936. https://doi.org/10.3389/fphar.2021.691936
26. Agarwal, H. (2020). Evaluation of in situ gel forming system loaded with etoricoxib and herbal adjuvant nanoparticles against human colon cancer cell lines (HT-29). *Letters in Applied NanoBioScience*, *9*(1), 789–795. https://doi.org/10.33263/lianbs0091.789795
27. Ibrahim, T. M., Ayoub, M. M., El-Bassossy, H. M., El-Nahas, H. M., & Gomaa, E. (2022). Investigation of Alogliptin-Loaded In Situ Gel Implants by 23 Factorial Design with Glycemic Assessment in Rats. *Pharmaceutics*, *14*(9), 1867. https://doi.org/10.3390/pharmaceutics14091867
28. Nair, A. B., Chaudhary, S., Shah, H., Jacob, S., Mewada, V., Shinu, P., … Shah, J. (2022). Intranasal Delivery of Darunavir-Loaded Mucoadhesive In Situ Gel: Experimental Design, In Vitro Evaluation, and Pharmacokinetic Studies. *Gels*, *8*(6), 342. https://doi.org/10.3390/gels8060342
29. Choudhary, S., Sharma, K., Bhatti, M. S., Sharma, V., & Kumar, V. (2022). DOE-based synthesis of gellan gum-acrylic acid-based biodegradable hydrogels: screening of significant process variables and *in situ* field studies. *RSC Advances*, *12*(8), 4780–4794. https://doi.org/10.1039/d1ra08786j
30. Bhute, H., Salve, P. S., Sheikh, S., Hussain, U. M., Tammewar, S., Tatode, A. A., … Premchandani, T. (2025). Development of a Gellan–Carbopol in Situ Gel System for Intranasal Delivery of Artemether-Loaded SLNs: Optimization and Kinetic Evaluation. *Journal of Pharmaceutical Innovation*, *21*(1). https://doi.org/10.1007/s12247-025-10263-6
31. RIYA V KALEBAR, PANKAJ GAJARE, MAMLE DESAI SN, VISHAL U KALEBAR, & RAVINDRANATH H ALADAKATTI. (2024). SYNERGISTIC DRUG COMPATIBILITY OF SUMATRIPTAN SUCCINATE AND METOCLOPRAMIDE HYDROCHLORIDE (IN SITU GEL FORMULATIONS) FOR NASAL DRUG RELEASE OPTIMIZATION. *Asian Journal of Pharmaceutical and Clinical Research*, *17*(3), 132–138. https://doi.org/10.22159/ajpcr.2024.v17i3.48485

32. El-Shenawy, A. A., Mahmoud, R. A., Mahmoud, E. A., & Mohamed, M. S. (2021). Intranasal In Situ Gel of Apixaban-Loaded Nanoethosomes: Preparation, Optimization, and In Vivo Evaluation. *AAPS PharmSciTech*, *22*(4), 147. https://doi.org/10.1208/s12249-021-02020-y
33. Khan, M. S., Ravi, P. R., Mir, S. I., & Rawat, P. S. (2023). Optimization and in vivo evaluation of triamcinolone acetonide loaded in situ gel prepared using reacted tamarind seed xyloglucan and kappa-carrageenan for ocular delivery. *International Journal of Biological Macromolecules*, *233*, 123533. https://doi.org/10.1016/j.ijbiomac.2023.123533
34. Adwan, S., Obeidi, T., & Al-Akayleh, F. (2024). Chitosan Nanoparticles Embedded in In Situ Gel for Nasal Delivery of Imipramine Hydrochloride: Short-Term Stage Development and Controlled Release Evaluation. *Polymers*, *16*(21), 3062. https://doi.org/10.3390/polym16213062
35. Salamanca, C. H., Barrera-Ocampo, A., Lasso, J. C., Camacho, N., & Yarce, C. J. (2018). Franz Diffusion Cell Approach for Pre-Formulation Characterisation of Ketoprofen Semi-Solid Dosage Forms. *Pharmaceutics*, *10*(3), 148. https://doi.org/10.3390/pharmaceutics10030148
36. Nijhawan, H. P., Vyas, J., Verma, P., & Yadav, K. S. (2025). Hyaluronic acid-coated cubosomal *in situ* gel for Brimonidine Tartrate: a sustained delivery system with enhanced ocular bioavailability and intraocular pressure reduction. *Journal of Biomaterials Science, Polymer Edition*, *37*(6), 1119–1152. https://doi.org/10.1080/09205063.2025.2543071
37. Zafar, A., Alsaidan, O. A., Imam, S. S., Yasir, M., Alharbi, K. S., & Khalid, M. (2022). Formulation and Evaluation of Moxifloxacin Loaded Bilosomes In-Situ Gel: Optimization to Antibacterial Evaluation. *Gels*, *8*(7), 418. https://doi.org/10.3390/gels8070418
38. Alhowyan, A. A., Kalam, M. A., Iqbal, M., Raish, M., El-Toni, A. M., Alkholief, M., … Alshamsan, A. (2023). Mesoporous Silica Nanoparticles Coated with Carboxymethyl Chitosan for 5-Fluorouracil Ocular Delivery: Characterization, In Vitro and In Vivo Studies. *Molecules*, *28*(3), 1260. https://doi.org/10.3390/molecules28031260
39. Guillot, A. J., Petalas, D., Skondra, P., Rico, H., Garrigues, T. M., & Melero, A. (2021). Ciprofloxacin self-dissolvable Soluplus based polymeric films: a novel proposal to improve the management of eye infections. *Drug Delivery and Translational Research*, *11*(2), 608–625. https://doi.org/10.1007/s13346-020-00887-1
40. Ginting, E. N. B., Lembang, G. V., Abdullah, D. A. P., Nurrakhma, S. S. R., Ridwan, Muh. R. I., & Permana, A. D. (2025). Validation of UV–Vis spectrophotometric colorimetric methods for Rifampicin quantification in PBS & biological matrices. *Bioanalysis*, *17*(9), 607–620. https://doi.org/10.1080/17576180.2025.2501942
41. Xia, H., Yang, J., Song, F., Pu, G., Dong, F., Liang, Z., & Zhang, J. (2024). Development of ion-triggered *in situ* gel containing ketoconazole/hydroxypropyl-β-cyclodextrin for ocular delivery: *in vitro* and *in vivo* evaluation. *Drug Delivery*, *31*(1), 2424217. https://doi.org/10.1080/10717544.2024.2424217
42. Jin, L., Li, X., Chen, X., Chen, X., Liu, Y., Xu, H., … Tang, Z. (2023). A study on puerarin in situ gel eye drops: Formulation optimization and pharmacokinetics on rabbits by microdialysis. *International Journal of Pharmaceutics*, *642*, 123176. https://doi.org/10.1016/j.ijpharm.2023.123176
43. Li, H., Anjani, Q. K., McGuckin, M. B., Himawan, A., Li, M., & Donnelly, R. F. (2023). Development of a HPLC fluorometric method for the quantification of enfuvirtide following in vitro releasing studies on thermosensitive in situ forming gel. *Drug Delivery and Translational Research*, *13*(8), 2183–2193. https://doi.org/10.1007/s13346-023-01344-5
44. Dong, Z., Dong, X., Wang, H., Pan, Y., Yang, M., Zhao, S., … Wang, S. (2026). Ion-Triggered In Situ Gel Combined with Melatonin Liposomes: Breaking Through the Dual Barriers of Nasal and Brain Delivery to Treat Insomnia.

Pharmaceutics, *18*(6), 656. https://doi.org/10.3390/pharmaceutics18060656

45. Teaima, M. H., Helal, D. A., Alsofany, J. M., El-Nabarawi, M. A., & Yasser, M. (2022). Ion-Triggered In Situ Gelling Intranasal Spray of Dronedarone Hydrochloride Nanocarriers: In Vitro Optimization and In Vivo Pharmacokinetic Appraisal. *Pharmaceutics*, *14*(11), 2405. https://doi.org/10.3390/pharmaceutics14112405
46. Balakrishnan, B., Sarojini, B. K., Kodoth, A. K., Dayananda, B. S., & Venkatesha, R. (2024). Fabrication and characterization of tamarind seed gum based novel hydrogel for the targeted delivery of omeprazole magnesium. *International Journal of Biological Macromolecules*, *258*(Pt 1), 128758. https://doi.org/10.1016/j.ijbiomac.2023.128758
47. GUPTA, N. V., SHANMUGANATHAN, S., KANNA, S., & SASTRI, K. T. (2021). A 23 FACTORIAL DESIGN FOR FORMULATION AND DEVELOPMENT OF DOXYCYCLINE HYDROCHLORIDE IN SITU GEL FORMING SOLUTION FOR WOUND HEALING APPLICATION. *International Journal of Applied Pharmaceutics*, *13*(3), 221–232. https://doi.org/10.22159/ijap.2021v13i3.39696
48. Cui, H., Xiong, Z., Ai, L., Xie, F., Song, Z., & Zhang, H. (2026). Characterization of EGCG-concentration responsive gel of tamarind seed polysaccharide. *Food Research International*, *228*, 118426. https://doi.org/10.1016/j.foodres.2026.118426
49. Sangnim, T., Limmatvapirat, S., Nunthanid, J., Sriamornsak, P., Sittikijyothin, W., Wannachaiyasit, S., & Huanbutta, K. (2018). Design and characterization of clindamycin-loaded nanofiber patches composed of polyvinyl alcohol and tamarind seed gum and fabricated by electrohydrodynamic atomization. *Asian Journal of Pharmaceutical Sciences*, *13*(5), 450–458. https://doi.org/10.1016/j.ajps.2018.01.002
50. Mandal, S., Das, N. R., Mukherjee, K., & Giri, T. K. (2025). *In vitro* , *ex vivo* , and *in vivo* evaluation of polysaccharide based thermo-sensitive *in situ* gel for the treatment of glaucoma. *Journal of Biomaterials Applications*, *40*(6), 650–665. https://doi.org/10.1177/08853282251369232
51. Hani, U., Rahamathulla, M., Osmani, R. A. M., Begum, M. Y., Wahab, S., Ghazwani, M., … Alqahtani, A. (2022). Development and Characterization of Oral Raft Forming In Situ Gelling System of Neratinib Anticancer Drug Using 32 Factorial Design. *Polymers*, *14*(13), 2520. https://doi.org/10.3390/polym14132520
52. Talantikite, M., Stimpson, T. C., Gourlay, A., Le-Gall, S., Moreau, C., Cranston, E. D., … Cathala, B. (2020). Bioinspired Thermoresponsive Xyloglucan–Cellulose Nanocrystal Hydrogels. *Biomacromolecules*, *22*(2), 743–753. https://doi.org/10.1021/acs.biomac.0c01521
53. Jabir, S. A., & Rajab, N. A. (2025). Preparation, In-vitro, Ex-vivo, and Pharmacokinetic Study of Lasmiditan as Intranasal Nanoemulsion-based In Situ Gel. *Pharmaceutical Nanotechnology*, *13*(1), 239–253. https://doi.org/10.2174/0122117385285009231222072303
54. Ranch, K. M., Maulvi, F. A., Naik, M. J., Koli, A. R., Parikh, R. K., & Shah, D. O. (2019). Optimization of a novel in situ gel for sustained ocular drug delivery using Box-Behnken design: In vitro, ex vivo, in vivo and human studies. *International Journal of Pharmaceutics*, *554*, 264–275. https://doi.org/10.1016/j.ijpharm.2018.11.016
55. Hirun, N., Kraisit, P., & Tantishaiyakul, V. (2022). Thermosensitive Polymer Blend Composed of Poloxamer 407, Poloxamer 188 and Polycarbophil for the Use as Mucoadhesive In Situ Gel. *Polymers*, *14*(9), 1836. https://doi.org/10.3390/polym14091836
56. Shaikh, D. A., & Momin, M. M. (2024). Formulation and Evaluation of Ion-Triggered In situ gel for Effective Ocular Delivery of Ciprofloxacin HCl and Olopatadine HCl in Combination. *Drug Delivery Letters*, *14*(1), 49–66. https://doi.org/10.2174/0122103031267809231128111259
57. Dholakia, M., Dave, R., Thakkar, V., Rana, H., Gohel, M., & Patel, N. (2018). NEWER OPHTHALMIC IN SITU GEL OF MOXIFLOXACIN HYDROCHLORIDE: OPTIMIZATION USING BOX BEHNKEN STATISTICAL DESIGN. *International*

Journal of Pharmacy and Pharmaceutical Sciences, *10*(12), 5. https://doi.org/10.22159/ijpps.2018v10i12.26979

58. Nair, A. B., Shah, J., Jacob, S., Al-Dhubiab, B. E., Sreeharsha, N., Morsy, M. A., … Venugopala, K. N. (2021). Experimental design, formulation and in vivo evaluation of a novel topical in situ gel system to treat ocular infections. *PLOS ONE*, *16*(3), e0248857. https://doi.org/10.1371/journal.pone.0248857

Figures

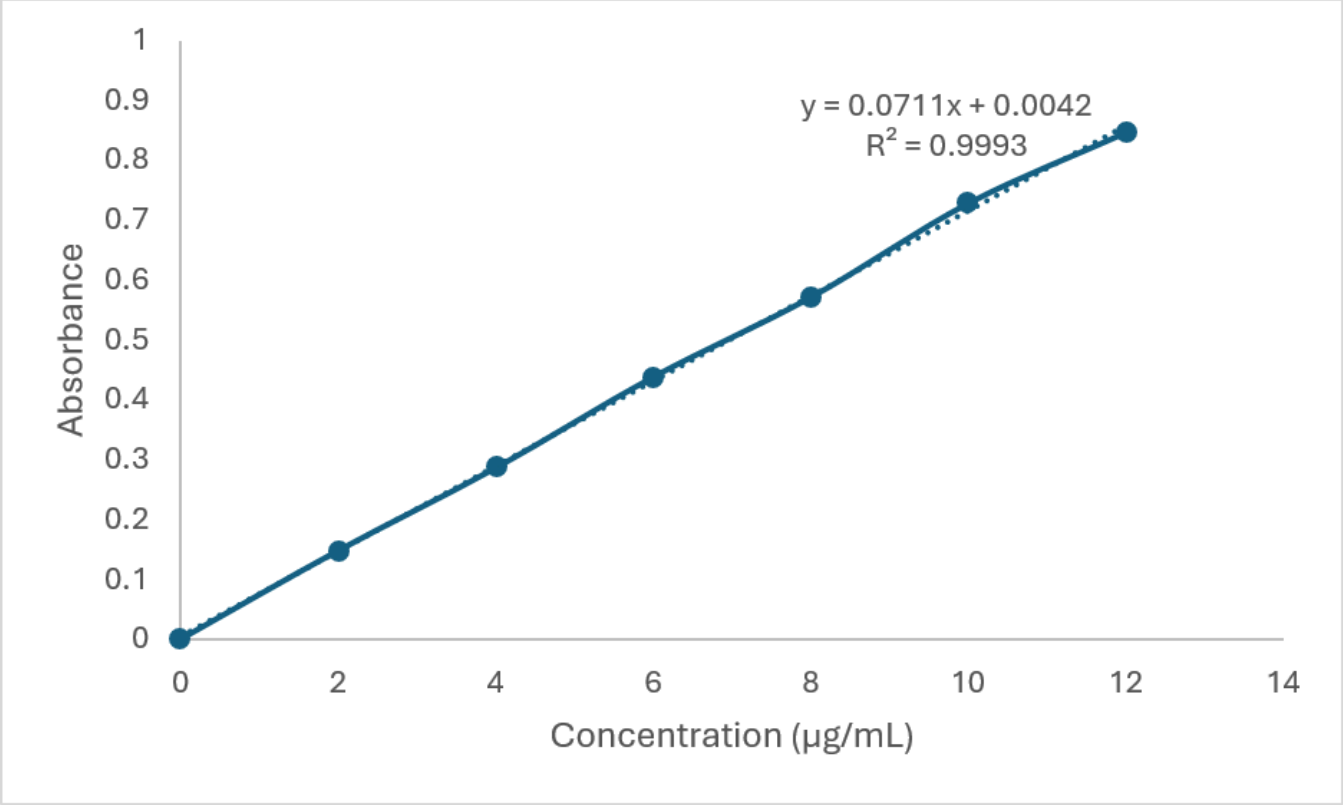


Figure 1

Calibration curve of puerarin at 250 nm.

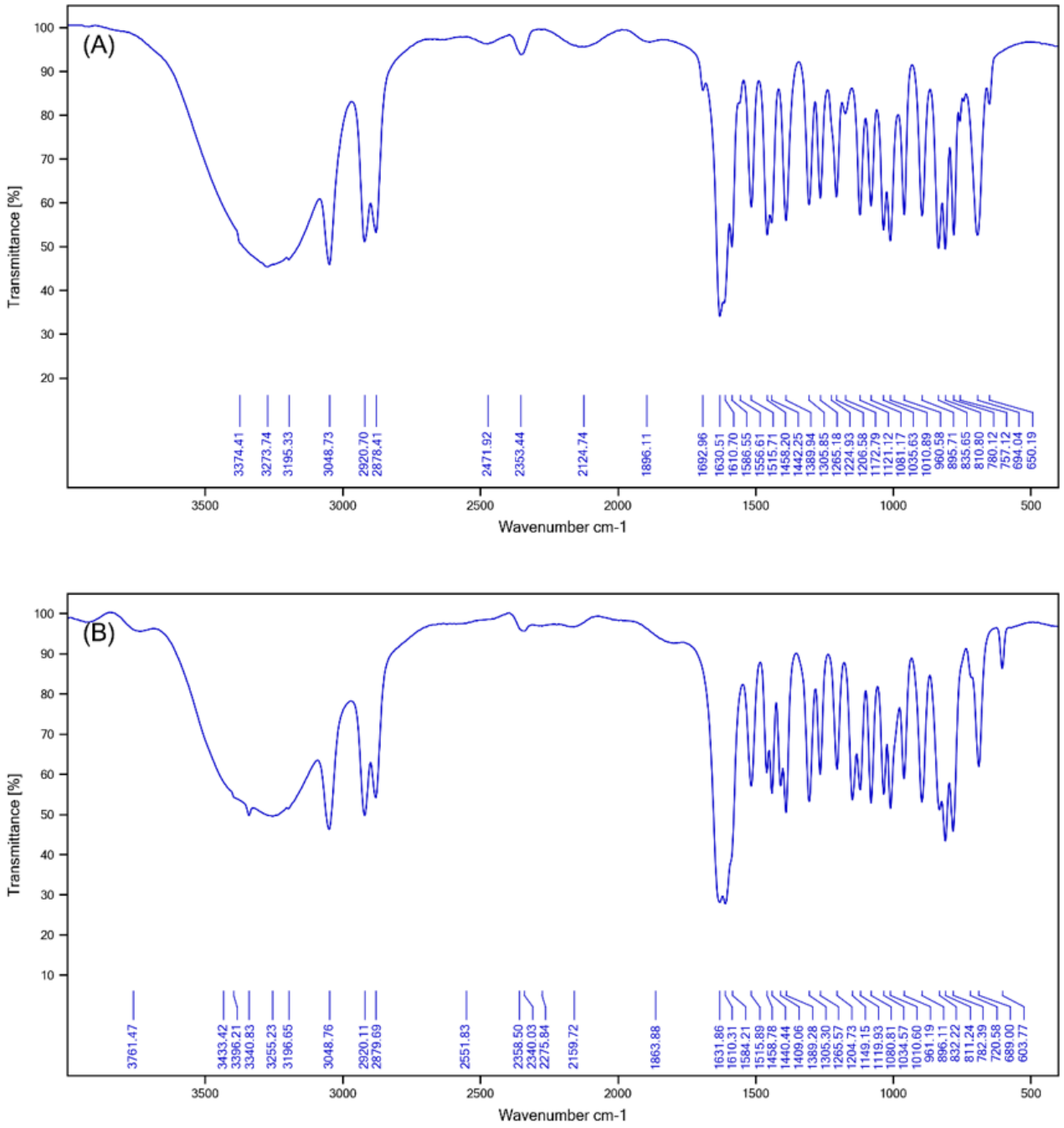


Figure 2

FTIR spectra of (A) pure puerarin and (B) physical mixture of puerarin with formulation excipients (gellan gum, tamarind seed xyloglucan, HPMC E4M, mannitol, disodium EDTA, and benzalkonium chloride).

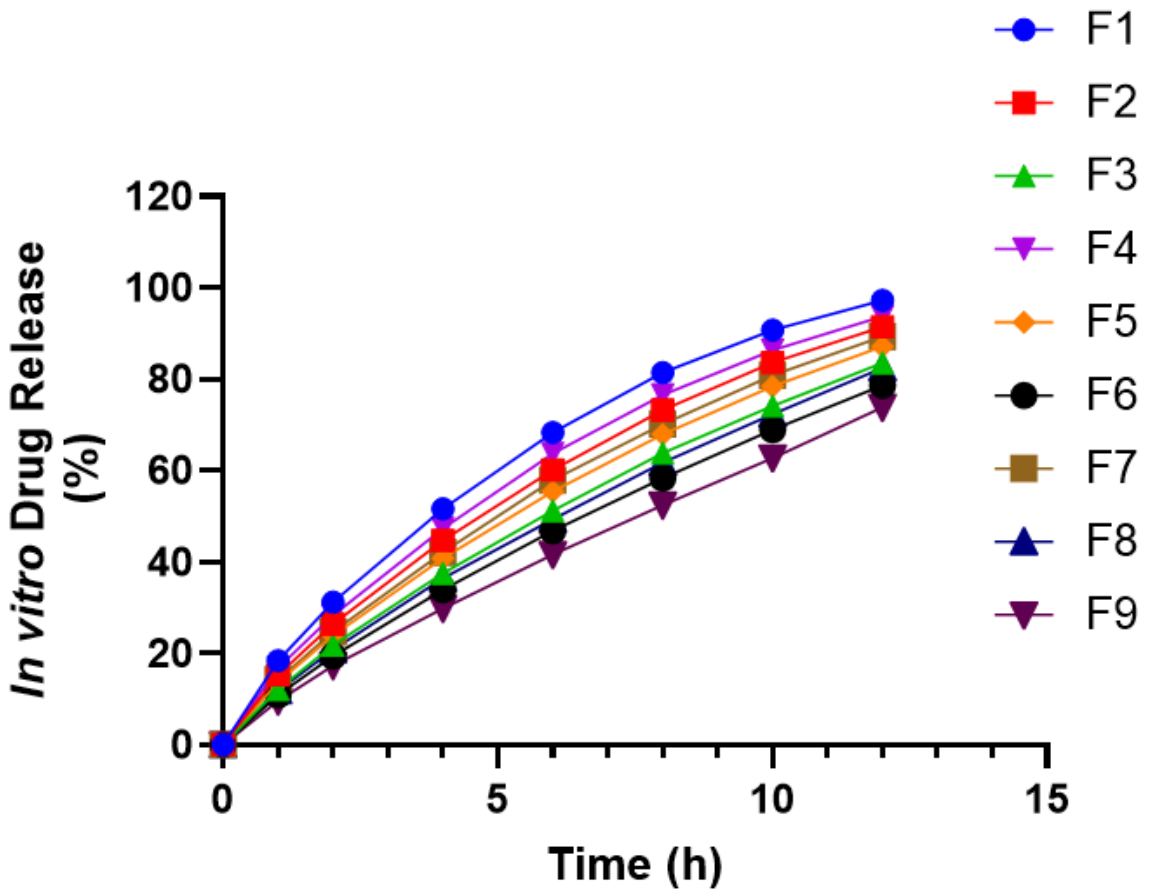


Figure 3

Cumulative In Vitro Drug Release (%) of Puerarin-Loaded Ion-Triggered In Situ Gel Formulations F1–F9 Across 12 h

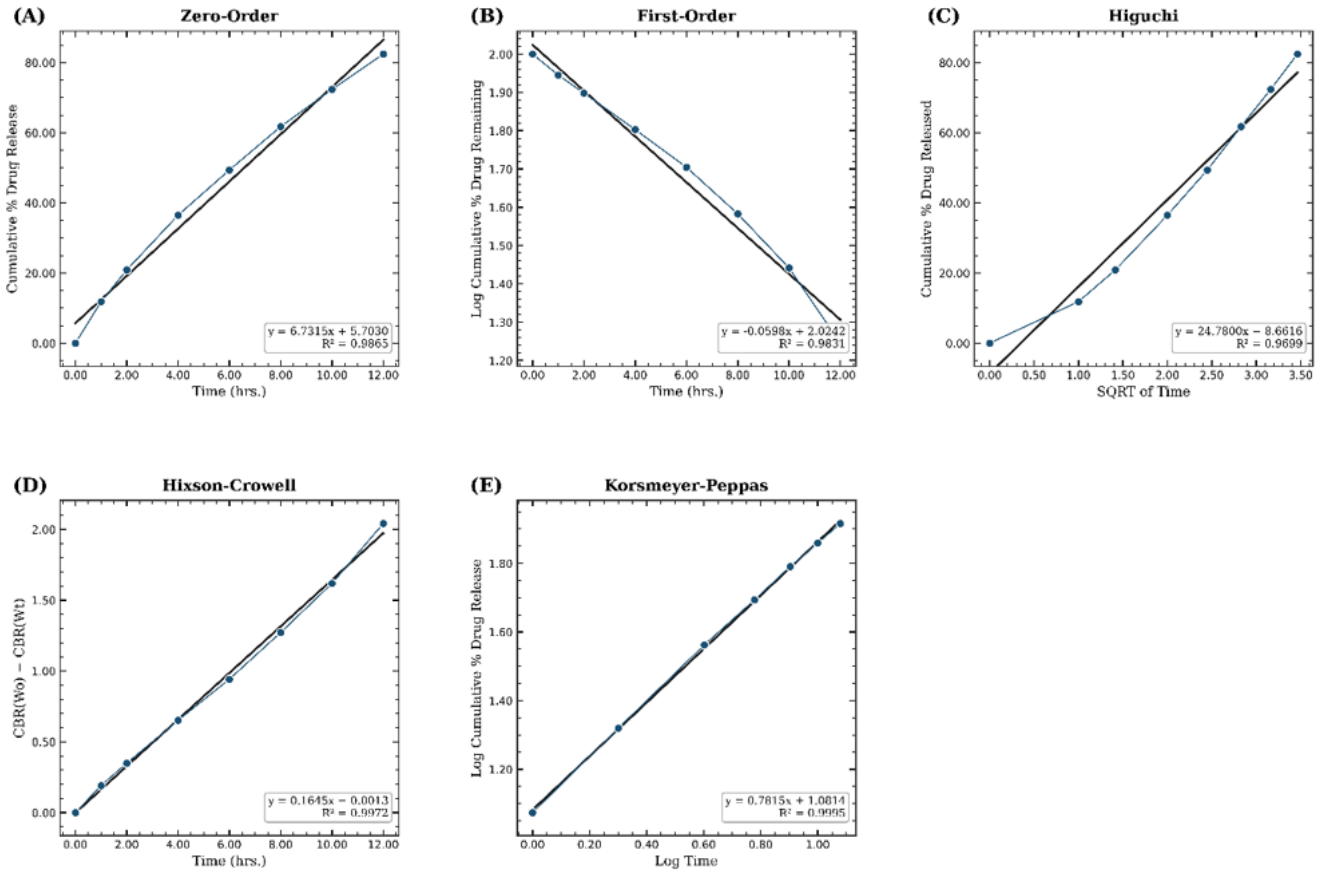


Figure 4

Release kinetics plots of optimized batch F8 (A) Zero-order, (B) First-order, (C) Higuchi, (D) Hixson-Crowell, and (E) Korsmeyer-Peppas models fitted to in vitro drug release data of puerarin-loaded ion-triggered in situ gel

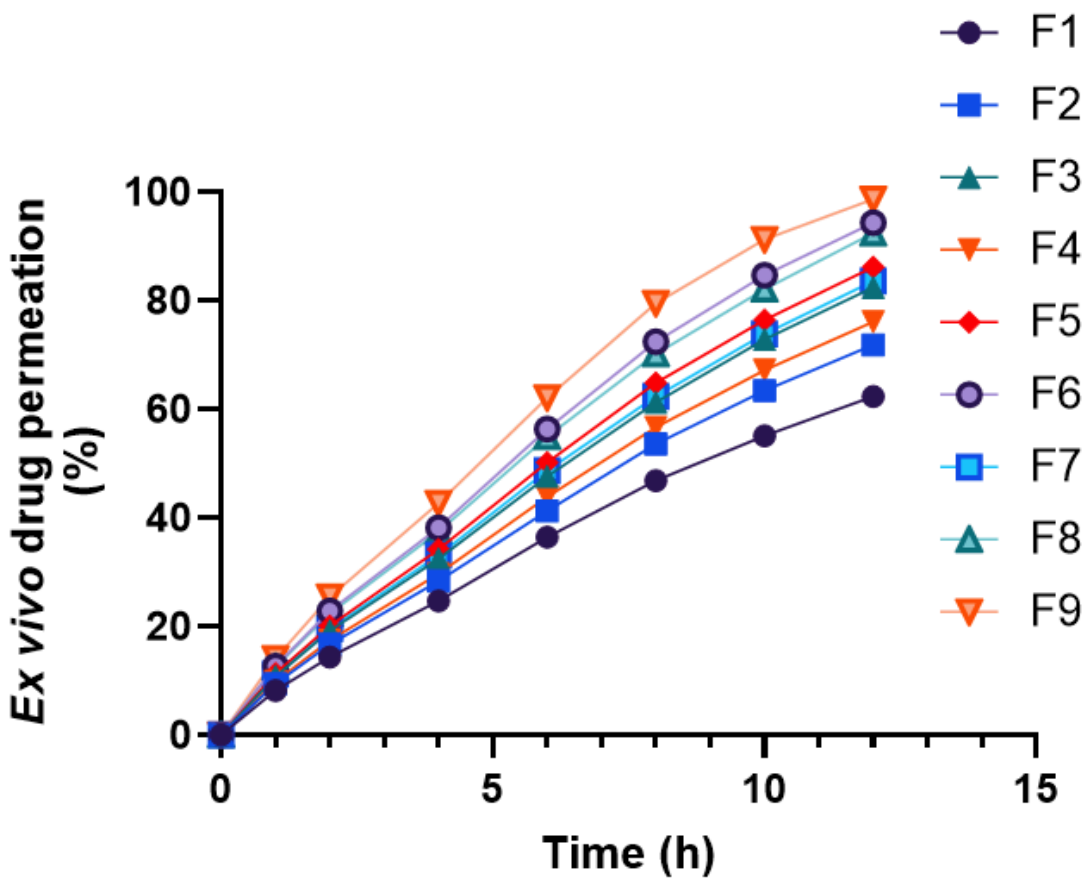


Figure 5

Cumulative *Ex Vivo* Corneal Permeation (%) of Puerarin-Loaded Ion-Triggered *In Situ* Gel Formulations F1–F9 Using Freshly Excised Goat Cornea

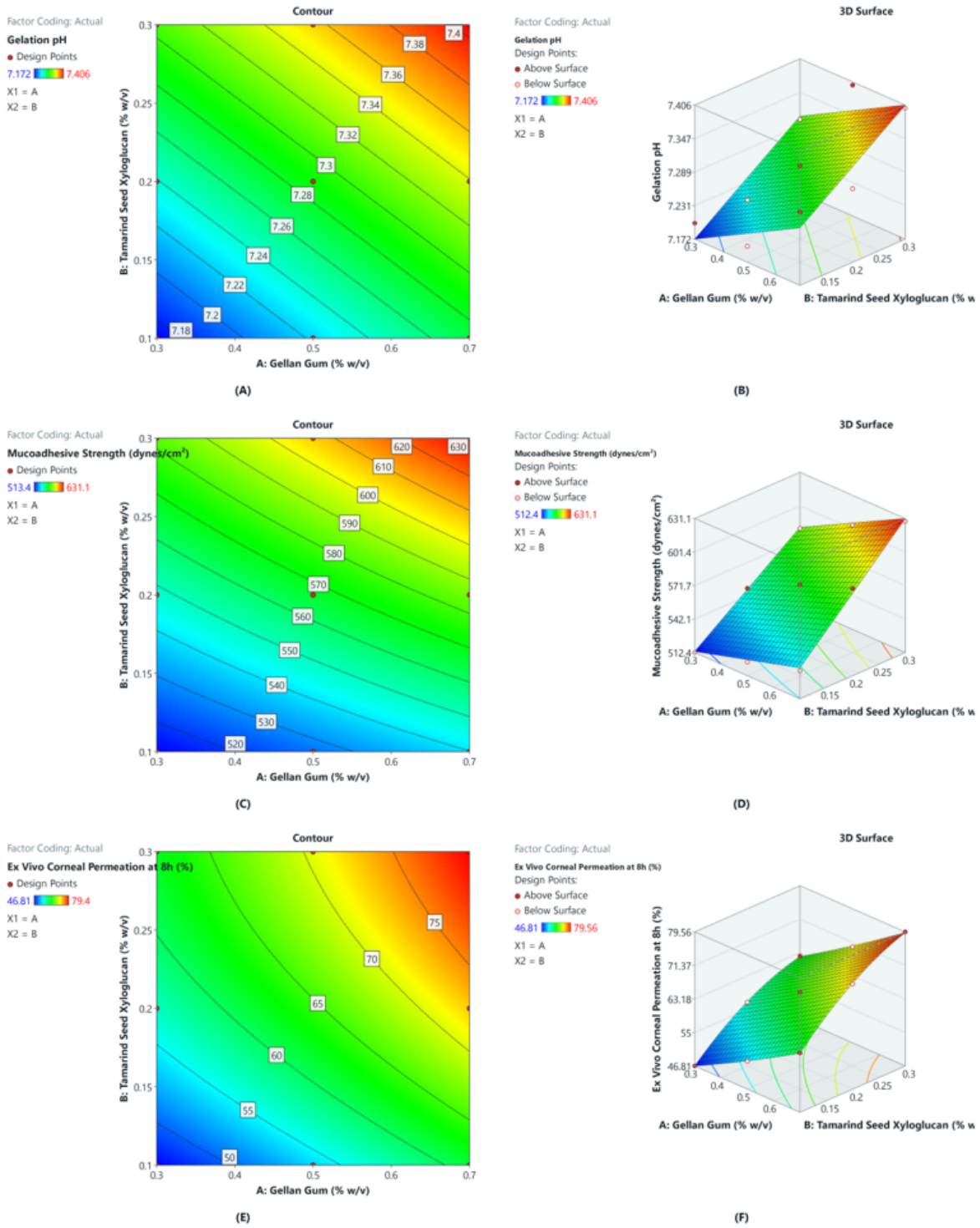


Figure 6

Two-dimensional contour plots and three-dimensional response surface plots illustrating the interactive effect of Gellan Gum and Tamarind Seed Xyloglucan on the measured responses. Plots (A–B) relate to gelation ph (Y_1): (A) two-dimensional contour plot showing the effect of Gellan Gum and Tamarind Seed Xyloglucan on Y_1; (B) three-dimensional response surface plot showing the effect of Gellan Gum and Tamarind Seed Xyloglucan on Y_1. Plots (C–D) relate to mucoadhesive strength (Y_2): (C) two-dimensional contour plot showing the effect of Gellan Gum and Tamarind Seed Xyloglucan on Y_2; (D) three-dimensional response surface plot showing the effect of Gellan

Gum and Tamarind Seed Xyloglucan on Y_2. Plots (E–F) relate to ex vivo corneal permeation at 8h (Y_3): (E) two-dimensional contour plot showing the effect of Gellan Gum and Tamarind Seed Xyloglucan on Y_3; (F) three-dimensional response surface plot showing the effect of Gellan Gum and Tamarind Seed Xyloglucan on Y_3.

Supplementary Files

This is a list of supplementary files associated with this preprint. Click to download.

- SupplementoryData.docx